Natural gas fugitive emissions rates constrained by global atmospheric methane and ethane

Stefan Schwietzke, W. Michael Griffin, H. Scott Matthews, and Lori M. P. Bruhwiler

Just Accepted

1 # Natural gas fugitive emissions rates constrained by

2 # global atmospheric methane and ethane

3 Stefan Schwietzke[*,†,♮], W. Michael Griffin[†,‡], H. Scott Matthews[†,§], Lori M. P. Bruhwiler[♯]

4 [†] Department of Engineering and Public Policy, Carnegie Mellon University, Baker Hall 129,

5 5000 Forbes Avenue, Pittsburgh, PA 15213, United States

6 [‡] Tepper School of Business, Carnegie Mellon University, 5000 Forbes Avenue, Pittsburgh, PA

7 15213, United States

8 [§] Department of Civil and Environmental Engineering, Carnegie Mellon University, Porter Hall

9 123A, 5000 Forbes Avenue, Pittsburgh, PA 15213, United States

10 [♯] NOAA Earth Systems Research Laboratory, 325 Broadway GMD1, Boulder, CO 80305,

11 United States

12 **Corresponding Author**

13 * Phone: (303) 497-5073. Fax: (303) 497-5590. E-mail: stefan.schwietzke@noaa.gov.

14 **Abstract**

15 The amount of methane emissions released by the natural gas (NG) industry is a critical and

16 uncertain value for various industry and policy decisions, such as for determining the climate

17 implications of using NG over coal. Previous studies have estimated fugitive emissions rates (FER)

18   – the fraction of produced NG (mainly methane and ethane) escaped to the atmosphere – between

19   1-9%. Most of these studies rely on few and outdated measurements, and some may represent only

20   temporal/regional NG industry snapshots. This study estimates NG industry representative FER

21   using global atmospheric methane and ethane measurements over three decades, and literature

22   ranges of (i) tracer gas atmospheric lifetimes, (ii) non-NG source estimates, and (iii) fossil fuel

23   fugitive gas hydrocarbon compositions. The modeling suggests an upper bound global average

24   FER of 5% during 2006–2011, and a most likely FER of 2-4% since 2000, trending downward.

25   These results do not account for highly uncertain natural hydrocarbon seepage, which could lower

26   the FER. Further emissions reductions by the NG industry may be needed to ensure climate

27   benefits over coal during the next few decades.

28   **Introduction**

29   The effectiveness of mitigating climate change using natural gas (NG) as a bridge to a renewable

30   energy-dominated economy has been challenged by some[1,2], suggesting that methane (CH_4)

31   emissions from NG systems could outweigh reduced CO_2 emissions compared to coal use. Other

32   studies[3–6] indicate that U.S. emissions inventories underestimate CH_4 emissions from the oil and

33   gas industry. The increased tapping of shale formations and other unconventional NG sources –

34   increasing production in North America and exploration activities worldwide using new

35   technologies – adds urgency to the problem.

36   The U.S. Environmental Protection Agency recently amended air regulations for the oil and gas

37   industry including targets for capturing NG that currently escapes to the atmosphere[7]. Accurately

38   determining CH_4 emissions that are representative of the NG industry is key for this and future

39   policies, but it is also challenging due to the size and complexity of the NG industry[8,9]. CH_4 is

40   released to the atmosphere, intentionally (e.g., venting) and unintentionally (leaks), throughout the

41   NG life cycle, which includes extraction, processing, transport, and distribution. The magnitude

42   of life cycle CH_4 emissions is sometimes reported as the NG fugitive emissions rate (FER), defined

43   here as the percentage of dry production – mainly CH_4 – that is lost throughout its life cycle.

44   Most literature FER estimates were generated using bottom-up approaches, i.e., aggregating

45   measurements and engineering estimates at different life cycle stages. Previous bottom-up studies

46   by these[10,11] and other authors[1,8,9] showed that outdated and small sample size measurement data

47   largely contribute to FER uncertainty. Local air sampling studies near NG production facilities

48   complement the bottom-up studies[3,4], but they only represent a regional and temporal snapshot of

49   the larger industry. High FER of 6-9% were reported recently using both approaches[1,4].

50   This work estimates global average FER with a top-down approach that uses long-term (1984-

51   2011) global atmospheric CH_4 and ethane (C_2H_6) measurements to evaluate the representativeness

52   of previous bottom-up results. These tracer gas species are the main hydrocarbon components of

53   NG[12]. Unlike CH_4, C_2H_6 is not thought to have microbial sources[13,14], so its atmospheric abundance

54   can be a useful constraint on FER. A third tracer – the carbon isotope $\delta^{13}C$-CH_4 – was employed,

55   which provides a stronger constraint for FER than CH_4 alone. $\delta^{13}C$-CH_4 observations[15] were used

56   to exploit the fact that the isotopic values of observed atmospheric CH_4 are the result of the

57   magnitudes and the distinct isotopic signatures of the various CH_4 sources. For instance, CH_4

58   emissions from fossil fuel (FF) sources are significantly less depleted in $\delta^{13}C$-CH_4 compared to

59   microbial sources, such as wetlands[16]. Previous top-down studies have estimated global or national

60   FF CH_4 and C_2H_6 emissions[5,13,17] using complex 3D models of the atmosphere based on (i) *a priori*

61   knowledge of the approximate locations of different emissions, and (ii) spatially distributed

62   atmospheric measurements. However, using observations to distinguish emissions from NG, oil,

63   and coal is difficult due to close relative proximity of these sources[6]. Quantifying the NG source

64   is necessary to estimate FER. A detailed global bottom-up oil and coal CH_4 and C_2H_6 emissions

65   inventory[18] was developed for this study to isolate NG emissions from those associated with oil

66   and coal.

67   **Methods**

68   Global NG CH_4 and C_2H_6 emissions and uncertainties were estimated annually over the period

69   1985-2011 using a top-down mass balance as the difference between total emissions and other

70   anthropogenic and natural sources. The mass balance model treats the global atmosphere as a

71   single box, which conserves the global mass of the emissions sources and sinks (and resulting

72   atmospheric mixing ratios), eliminating the need for complex global transport of emissions. Total

73   annual emissions ranges were based on (i) CH_4 and C_2H_6 atmospheric measurement data from

74   NOAA's[19] and UC-Irvine's[13] global observation networks (see SI section 1 for global average

75   annual mixing ratios), respectively, (ii) literature atmospheric $\delta^{13}C$-CH_4 data[15], and (iii) literature

76   ranges of global average atmospheric CH_4 and C_2H_6 lifetimes (both largely dependent on reaction

77   with OH)[20–24] summarized in the following subsection. The magnitudes of the uncertain

78   anthropogenic and natural CH_4 and C_2H_6 sources were derived using a wide range of literature

79   estimates (SI section 2) and the above-mentioned oil and coal inventory[18]. Given the resulting

80   annual NG CH_4 and C_2H_6 top-down estimates, FER was estimated using global NG production

81   statistics in combination with thousands of NG composition samples specifying NG CH_4 and C_2H_6

82   contents worldwide.

83   Inter-annual variability in the OH abundance and the non-FF source strength affects FER

84   estimates in a given year. For instance, declining OH or non-FF emissions would increase FER.

85   This study is primarily interested in the long-term FER trajectory. We therefore only accounted

86   for inter-annual variations in the above model parameters where the literature indicates a long-

87   term trend (such as in CH_4 and C_2H_6 mixing ratios shown in SI section 1). Given the lack of

88   evidence for long-term trends in the global OH abundance[25] and non-FF emissions[13,17] (for details

89   see SI sections 1 and 2, respectively), inter-annual variation in non-FF emissions sources was

90   neglected.

91   Using a relatively simple model, a range of scenarios was explored in order to evaluate what

92   may be learned from the atmospheric observations, including the maximum possible global

93   average FER. Finally, mass balance FER estimates were substantiated using the existing 3D global

94   chemistry transport model TM5[26] implemented in the CarbonTracker-CH_4 (CT-CH_4) assimilation

95   system[27]. This was achieved by simulating transport of emissions throughout the global

96   atmosphere for selected FER scenarios. The resulting CH_4 mixing ratios were then compared with

97   observations from the global networks[13,19], thereby adding spatial information not available using

98   the mass balance model.

99   **Global mass balance (box-model)**

100   The global annual mass balance for CH_4 and C_2H_6 in year t was formulated as:

101

$$z_{CH4,t} = z_{CH4,t,AgW} + z_{CH4,t,Nat} + z_{CH4,t,BBM} + z_{CH4,t,Oil} + z_{CH4,t,NG} + z_{CH4,t,Coal/Ind}$$ **Eq. 1,**

$$z_{C2H6,t} = z_{C2H6,t,BBE} + z_{C2H6,t,BFC} + z_{C2H6,t,Oil} + z_{C2H6,t,NG} + z_{C2H6,t,Coal}$$ **Eq. 2,**

102

103   where $z_{CH4,t}$ and $z_{C2H6,t}$ are the total annual global CH_4 and C_2H_6 emissions, respectively. The CH_4

104   emissions sources include agriculture/waste/landfills (*AgW*), natural sources (*Nat*), biomass

105   burning methane (*BBM*), oil life cycle fugitive emissions (*Oil*; CH_4 and C_2H_6), NG life cycle

106   fugitive emissions (*NG*; CH_4 and C_2H_6), and coal life cycle fugitive and "other energy and

107   industry" emissions (*Coal/Ind*). The C_2H_6 emissions sources also include biomass burning ethane

108   (*BBE*; savanna and grassland fires, tropical and extratropical forest fires, agricultural residue

109   burning), biomass fuel combustion (*BFC*), and coal life cycle C_2H_6 emissions (*Coal*; see below for

110   "other energy and industry" C_2H_6 emissions). The literature-based CH_4 and C_2H_6 emissions ranges

111   are summarized in the Methods subsections (non-FFs and FFs) below. The system boundaries for

112   the CH_4 sources vary slightly among studies, but are largely consistent with those described for

113   modeling with TM5 (SI Table S1). Mass balances were solved for $z_{CH4,t,NG}$ and $z_{C2H6,t,NG}$

114   independently using the ranges for all other source categories. The annual emissions $z_{CH4,t}$ were

115   estimated using Eq. 4, which is the solution to differential Eq. 3, giving $z_{CH4,t}$. The annual emissions

116    $z_{C2H6,t}$ were estimated using Eq. 5:

117

$$dC_{CH4}/dt = z_{CH4,t} - 1/\tau * C_{CH4,t}$$
Eq. 3,

$$z_{CH4,t} = \left(C_{CH4,t} - C_{CH4,t-1} * e^{-\frac{1}{\tau}} \right) * \left(\tau * \left(1 - e^{-\frac{1}{\tau}} \right) \right)^{-1}$$
Eq. 4,

$$z_{C2H6,t} = C_{C2H6,t} * SF_{C2H6}$$
Eq. 5,

118

119   where $C_{CH4,t}$ is the annually observed global average CH_4 dry air mole fraction (in ppb) in year t

120   multiplied by the conversion factor 2.767 Tg CH_4/ppb[28] in order to convert mole fractions to mass

121   units for the global atmosphere (see SI section 1 for details). For the global average atmospheric

122   lifetime of CH_4, τ, a range of 9.1-9.7 years was chosen, which includes the mean values from four

123   recent studies[20–23]. The scaling factor SF_{C2H6} converts the annually observed global average C_2H_6

124   dry air mole fraction $C_{C2H6,t}$ into the annual emissions burden $z_{C2H6,t}$, which is based on 3D-

125   modeling[24] and has been applied recently elsewhere[13]. Given uncertainties of up to 45% due to the

126   reaction rate with and mixing ratios of OH[24], the average and upper bound values of SF_{C2H6}

127   (corresponding to a higher global budget for estimating upper bound FER), 0.018 and 0.026 Tg

128   C_2H_6/ppt, respectively, were used.

129   The global mass balance using atmospheric δ^{13}C-CH$_4$ measurements constrains FER based on

130   the fact that the various CH$_4$ sources carry distinct isotopic CH$_4$ signatures. The ^{13}C:^{12}C ratio of

131   CH$_4$, δ (in ‰), can be expressed as[29]:

132

$$\delta = \left(R_{Sample}/R_{Standard} - 1\right) * 1000$$
<div align="right">**Eq. 6,**</div>

133

134   where $R = \textit{(Rare isotope / Abundant isotope)}$. The global mass balance for three CH$_4$ source

135   categories can be formulated for each year as[16]:

136

$$z_{CH4,t} = z_{Mic,t} + z_{FF,t} + z_{BBM,t}$$
<div align="right">**Eq. 7,**</div>

$$\delta_q z_{CH4,t} = \delta_{Mic} * z_{Mic,t} + \delta_{FF} * z_{FF,t} + \delta_{BBM} * z_{BBM,t}$$
<div align="right">**Eq. 8,**</div>

137

138   where $z_{Mic,t}$, $z_{FF,t}$, and $z_{BBM,t}$ refer to the microbial, FF, and BBM fraction of total annual CH$_4$

139   emissions, respectively, and $z_{Mic,t}$ includes all natural and agriculture/waste/landfills sources. The

140   different CH$_4$ emissions sources are aggregated to only three emissions categories in order to avoid

141   an under-constrained system of two linear equations (Eq. 7 and Eq. 8). The equation system is

142   solved for $z_{Mic,t}$ and $z_{FF,t}$ as an optimization problem (Eq. 10 through Eq. 15), and $z_{BBM,t}$ is

143   considered at least 25 Tg CH$_4$/yr (see literature review in SI section 2). The literature provides

144   wide ranges of source- (and geography-) specific isotopic signatures. For instance, Finnish

145   subarctic wetlands range between –65 ‰ and –69 ‰[30] compared to –51 ‰ and –53 ‰ from

146   landfills[16]. West Siberian NG associated with oil production (high CH$_4$ content) has been measured

147   around -50 ‰[30], whereas mature dry gas can range approximately -20 ‰[31]. The isotopic signatures

148   δ_{Mic}, δ_{FF}, and δ_{BBM} in this model are based on weighted averages of each emissions category from

149   13 literature sources[16], and lie within the range of –59 to –63 ‰, –38 to –42 ‰, and –22 to –26

150 ‰, respectively. The total annual CH4 emissions burden $z_{CH4,t}$ is the same as in Eq. 4, and the flux

151 weighted mean isotopic ratio of all CH4 sources[29] is:

152

$$\delta_{q,t} = \alpha\delta_a + \varepsilon - \frac{\varepsilon(1 + \delta_a/1000)}{z_{CH4,t}} * \frac{dC_{CH4,t}}{dt} + \frac{d\delta_a}{dt} * \frac{C_{CH4,t}}{z_{CH4,t}}$$ **Eq. 9**,

153

154 where $\alpha = (1 + \varepsilon / 1000)$ is the isotopic fractionation factor associated with photochemical CH4

155 destruction, for which $\varepsilon = -6.3$ ‰[16]. As described in more detail in SI section 1, the global annual

156 means of measured δ_a range between -47.0 ‰ and -47.3 ‰ throughout 1988–2011[15,32,33]. Given

157 (i) the lack of pre–1988 data, (ii) the reliance on unpublished post-2006 data[32], (iii) and the low

158 sensitivity of the above δ_a range on FER (see SI section 3.1), this model assumes a constant δ_a of

159 -47.1 ‰. Eq. 7 and Eq. 8 were re-arranged to give:

160

$$z_{FF,t} = \frac{\delta_{q,t} * z_{CH4,t} - \delta_{Mic} * (z_{CH4,t} - z_{BBM,t}) - \delta_{BBM} * z_{BBM,t}}{\delta_{FF} - \delta_{Mic}}$$ **Eq. 10**,

$$z_{Mic,t} = z_{CH4,t} - z_{FF,t} - z_{BBM,t}$$ **Eq. 11**,

161

162 where units for $z_{CH4,t}$ and δ are Tg CH4/yr and ‰, respectively. The optimization problem is to

163 minimize Eq. 10, such that:

164

$$z_{BBM,t} \geq 25$$ **Eq. 12**,

$$-59 \geq \delta_{Mic} \geq -63$$ **Eq. 13**,

$$-38 \geq \delta_{FF} \geq -42$$ **Eq. 14**,

$$-22 \geq \delta_{BBM} \geq -26$$ **Eq. 15**.

165

166   Eq. 12 ensures that there are only two unknowns in the problem of two linear equations. CH_4

167   emissions from NG $z_{C13CH4,t,NG}$ (based on isotope observations) are the difference between FF

168   emissions from the isotope mass balance and coal/oil emissions, which are described in more detail

169   below:

170

$$z_{C13CH4,t,NG} = z_{FF,t} - z_{CH4,t,Coal/Ind} - z_{CH4,t,Oil}$$ **Eq. 16**.

171

172   Finally, FER is estimated using Eq. 17 through Eq. 19:

173

$$FER_{CH4,t} = z_{CH4,t,NG}/\left(P_{dry,t} * WF_{down,CH4,t}\right)$$ **Eq. 17,**

$$FER_{C2H6,t} = z_{C2H6,t,NG}/\left(P_{dry,t} * WF_{down,C2H6,t}\right)$$ **Eq. 18,**

$$FER_{C13CH4,t} = z_{C13CH4,t,NG}/\left(P_{dry,t} * WF_{down,CH4,t}\right)$$ **Eq. 19,**

174

175   where $P_{dry,t}$ is the global dry production of NG[34] converted from volume to weight units (see our

176   bottom-up inventory[18] for details), and $WF_{down,CH4,t}$ and $WF_{down,C2H6,t}$ are the downstream NG

177   weight fractions of CH_4 and C_2H_6, respectively.

178   **Global 3D model**

179   Three-dimensional forward simulations of CH_4 emissions using the global chemistry transport

180   model TM5[26] complement the box-model approach. Forward simulations in this work cover the

181   period 1989-2011, and measurements are the same as used for the box-model. The following five

182   different zones were distinguished in order to analyze the spatial differences ignored in the box-

183   model: polar Northern Hemisphere (PNH, 53.1°N-90°N), temperate Northern Hemisphere (TNH,

184   17.5°N-53.1°N), the tropics (17.5°S-17.5°N), temperate Southern Hemisphere (TSH, 17.5°S-

185   53.1°S), and polar Southern Hemisphere (PSH, 53.1°S-90°S). These zones are pre-defined in CT-

186 $CH_4{}^{27}$, and briefly discussed in SI section 3.2. Emissions were simulated for 11 individual CH_4

187 source/sink categories including NG, oil, coal/industry, wetlands, soils, oceans, termites, wild

188 animals, agriculture/waste/landfills, and biomass burning methane (all as described above).

189 Emissions were simulated for each source separately, which allows tracking the individual

190 contributions of total CH_4 mixing ratios. Estimating source-specific contributions is key for

191 analyzing the underlying causes of potential spatial differences between simulations and

192 observations. These spatial differences mainly occur because the various sources emit in specific

193 world regions, which helps to distinguish emissions sources using the measurements from the

194 global monitoring networks.

195 **Model values of non-fossil fuel emissions categories based on literature review**

196   This section describes the range of non-NG CH_4 and C_2H_6 emissions values chosen as inputs in

197 the box-model (Eq. 1, Eq. 2, Eq. 10, and Eq. 11) and the 3D-model. Non-FF CH_4 emissions ranges

198 were selected based on five of the most recent inversion studies[27,35–38] and two literature

199 reviews[39,40], which is described in more detail in the SI (section 2), and summarized in Table 1. In

200 the box-model, most likely FER assumes total non-FF CH_4 sources of 400 Tg/yr (medium non-FF

201 scenario), and upper bound FER is associated with non-FF CH_4 sources of 265 Tg/yr (low non-FF

202 scenario). The corresponding medium and low scenario C_2H_6 estimates are 5.9 Tg/yr and 2.2

203 Tg/yr, respectively. High CH_4 and C_2H_6 scenarios were selected such that low and high values

204 represent a normal distribution around the medium values. Three-dimensional forward simulations

205 were carried out with TM5 for 8 individual non-FF CH_4 source/sink categories (totaling on average

206 385 Tg/yr). The global soil CH_4 sinks used in both models cover the range of literature values: 25

207 Tg/yr[36], 30 Tg/yr[35], and 38 Tg/yr[38]. The total non-FF emissions in the 3D simulation and in the

208 medium box-model scenario are very similar (difference is ~3% of global CH_4 budget), which

209   allows direct comparison of box-model results with the 3D-model (the same oil and coal estimates

210   were used in both models).

211

212   **Table 1:** Summary of global non-FF emissions estimates used in 3D-forward-modeling (TM5)

213   and ranges for box-modeling. Units are Tg/yr.

			CH_4				C_2H_6		
		Natural	**Ag/waste/ landfills**	**BBM**	**Soil sink [i]**	**Total**	**BBE**	**BFC**	**Total**
Box-model (const. over time [ii])									
	low	130	130	25	-25	260	1.6	0.6	2.2
	medium	182	200	43	-25	400	3.6	2.3	5.9
	high	235	270	60	-25	540	5.2	4.0	9.2
3D-model (avg. 1980-2011)		215 [iii]	194 [iv]	16 [v]	-40	385	n/a	n/a	n/a

214   Notes: Ag – Agriculture; BBM - Biomass burning methane; BBE - Biomass burning ethane;
215   BFC - Biomass fuel combustion; [i] Box-model data from[17], 3D-model data from[41]; [ii] Inter-annual
216   variations during 1980-2011 were ignored due to lack of long-term trends in OH and non-FF
217   sources, and focus on long-term FER trajectory (see also text above); [iii] Annual emissions and
218   seasonal cycle from[42]; [iv] Annual emissions from[43], seasonal cycle from[44]; [v] Annual emissions
219   from[45,46], seasonal cycle from[47].

220

221   **Model values of fossil fuel emissions categories from bottom-up inventory**

222   This section briefly summarizes the methods and data used to estimate CH_4 and C_2H_6 emissions

223   from oil and coal production, processing and transport (in Eq. 1 and Eq. 2) as well as downstream

224   NG composition (Eq. 17 through Eq. 19) applied in the box-model and the 3D-model. This

225   summary is based on a global bottom-up FF inventory developed by these authors[18]. Here, only

226   the general methodology and major parameters are reviewed. The inventory is based on country-

227   level NG, oil, and coal production data[34], a range of literature emissions factors (EFs, see below

228   for literature sources), and observational gas flaring data[48,49]. EFs describe the amount of

229   hydrocarbon gas emitted to the atmosphere per unit of fuel produced, and EFs are the basis for

230   comparing greenhouse gas (GHG) emissions among different fuels or technologies in life cycle

231   assessment. The inventory also includes hydrocarbon composition data from thousands of samples

232   including NG and oil wells, both of which produce NG and oil[12]. The hydrocarbon composition

233   data is necessary for deriving FER from estimated total amounts of global NG CH_4 ($z_{CH4,t,NG}$) and

234   C_2H_6 ($z_{C2H6,t,NG}$) emissions.

235   Emissions factors (EF) related to the oil life cycle were reviewed from four studies[50–53], which

236   span an order of magnitude. The EFs include fugitive emissions from oil production, processing,

237   and shipping as well as hydrocarbon emissions from incompletely flared gas. The EF selected from

238   these studies[51] is 50% below the mean of the lowest[52,53] and highest[50] literature EF. This selection

239   assures that the upper bound FER from the box-model is a conservative estimate, i.e., box-model

240   FER could be lower if oil emissions were in fact higher. Emissions from marketed (i.e., not

241   flared/vented or repressured) associated NG production at oil wells are counted towards FER. The

242   detailed procedure for allocating emissions between oil and NG production is described in the

243   bottom-up inventory[18]. Country-specific EFs related to the coal life cycle[50,54–56] distinguish

244   different types of coal production. Comparison of different global coal production estimates (and

245   Chinese coal production in particular) suggests that the total emissions estimate in the inventory

246   may be an underestimate. Thus, analogously to the oil emissions estimates above, FER could be

247   lower than box-model results if coal emissions were in fact higher.

248   Table 2 summarizes the results from the bottom-up inventory[18] including oil and coal CH_4 and

249   C_2H_6 emissions over different time periods as well as global average downstream NG hydrocarbon

250   composition (related to dry production statistics). Medium oil CH_4 emissions increase from 14

251   Tg/yr (mean during 1985-1999) to 17 Tg/yr (mean during 2006-2011), and medium coal/industry

252 CH_4 emissions increase from 48 Tg/yr to 61 Tg/yr over the same periods. Medium oil C_2H_6

253 emissions increase from 5.5 Tg/yr to 6.6 Tg/yr over the same periods, and coal/industry C_2H_6

254 emissions are relatively small given the low coal-bed gas C_2H_6 content[18]. Downstream NG CH_4

255 and C_2H_6 contents averaged throughout 1984-2011 range from 85-87 wt-% and 7.2-7.7 wt-%,

256 respectively, while C_2H_6 content decreased from 7.8–6.8 wt-% over this period due to increased

257 C_2H_6 extraction for NG liquids[18].

258

259 **Table 2:** Summary of oil and coal/industry CH_4 and C_2H_6 emissions, and downstream NG

260 composition in the bottom-up inventory[18].

		Units	CH$_4$			C$_2$H$_6$ [i]		
			1985-1999	2000-2005	2006-2011	1985-1999	2000-2005	2006-2011
Emissions								
	low		5	6	6	4.4	5.0	5.2
Oil	medium		14	16	17	5.5	6.3	6.6
	high	Tg/yr	41	48	51	7.6	8.8	9.2
	low		43	44	55	0.0	0.0	0.0
Coal/Industry	medium		48	49	61	0.3	0.3	0.4
	high		56	57	71	0.6	0.6	0.8
Composition								
	low			85			7.2	
Downstream NG [ii]	medium	wt-%		86			7.4	
	high			87			7.7	

261 Notes: [i] Ranges of oil and coal/industry C_2H_6 emissions are due to uncertainties in C_2H_6 content
262 of fugitive hydrocarbon emissions. [ii] Downstream NG composition was estimated for use with dry
263 production statistics (shows averages over 1985-2011) to estimate life cycle FER (as described
264 above). Results are based on a mass balance of upstream NG, downstream NG, and natural gas
265 liquids at the processing stage (see box-model Methods). Low and high values represent 95%-C.I.

266

267 Industry (public power and heat, other energy industries, transportation, residential and other

268 sectors, industrial processes, FF fires) emissions were adopted from EDGAR v4.2[43]. C_2H_6

269 emissions estimates from this source were unavailable, and were not accounted for in the box-

270 model. FER could in fact be lower than box-model results if industry is a significant C_2H_6 source.

271   Three different FER scenarios (ranging from 2-6% FER; see SI for details) were simulated in TM5

272   to analyze which FER is most consistent with spatially distributed observations.

273   **Spatial distribution of CH$_4$ emissions**

274   Spatial CH$_4$ emissions grid maps were developed in order to perform 3D simulations of the

275   global atmosphere in TM5. A detailed description of the grid map development as well as the

276   results is provided in the bottom-up inventory[18], and briefly summarized here. The spatial

277   distribution of FF emissions *within* each country was adopted from EDGAR v4.2[43], which is based

278   on population density and other proxies. The absolute FF emissions in the grid maps were scaled

279   based on the FF estimates summarized in the previous subsection. Due to the emissions differences

280   between this work and EDGAR for a given country, the spatial distribution of the scaled grid maps

281   differs from EDGAR on a global scale, but not within individual countries. In contrast to FF, other

282   source categories have a distinct seasonal emissions cycle. EDGAR's agriculture/waste/landfills

283   category annual emissions grid maps were decomposed into monthly grid maps, and scaled to a

284   seasonal cycle as defined in SI Table S1. Agriculture/waste/landfills annual totals were linearly

285   extrapolated from 2008 (last year in EDGAR) to 2011 using the last 10 years available in EDGAR.

286   Literature spatial CH$_4$ emissions distribution was adapted for natural[57,58] and BBM[47] categories.

287   **Results**

288   Global average FER from the NG life cycle was estimated in a top-down approach to better

289   understand industry representative CH$_4$ emissions. This study is based on global spatially

290   distributed CH$_4$, δ^{13}C-CH$_4$, and C$_2$H$_6$ measurements over three decades. A global box-model was

291   developed and an existing 3D emissions transport model was used to attribute total emissions to

292   different sources, thereby taking into account uncertainties in atmospheric lifetimes of measured

293   species as well as non-NG source estimates.

Global box-model

295   The most likely global FER of 2-4% on average during 2004-2011 (Figure 1) is consistent for

296   CH_4, $\delta^{13}C$-CH_4, and C_2H_6 observations. These estimates assume (i) mean literature emissions

297   values for each of the other source categories listed above, and (ii) global total oil and coal CH_4

298   emissions from this study's emissions inventory (medium values in Table 2), which agree well

299   (2.5% difference) with EDGAR[43], i.e., the commonly used *a priori* FF database in global top-

300   down CH_4 modeling. The upper bound global FER averaged over the last five years of observations

301   is 5.0% (4.4% in 2011) based on C_2H_6 observations (Figure 1). The upper bound assumes (i) a

302   C_2H_6 lifetime corresponding to the largest global average sink in the literature, (ii) a lower bound

303   FF C_2H_6 content (Table 2), and (iii) a lower bound BBE/BFC C_2H_6 source estimate (Table 1).

304   Details of the budgetary implications of the upper bound FER relative to the literature are

305   illustrated in SI Figure S8. Results indicate upper bound FER of ~6% in the early 2000s, mainly

306   due to lower FF production compared to later years. Note that FER peaks shown for some years

307   in Figure 1 are likely due to inter-annual variation in natural sources[13]. Our upper bound throughout

308   1985-1999 is on average 9.3% (SI Figure S7). This temporal decline in FER is consistent with

309   earlier work suggesting a decrease in FF C_2H_6 emissions[13,14]. Emissions reductions per unit of

310   production (FER) in this work imply industry efficiency improvements, although the decline

311   would be less steep if coal and oil EFs also declined over time (increased oil and coal production

312   over time are accounted for). Global average CH_4 and $\delta^{13}C$-CH_4 data provide weaker constraints

313   for upper bound FER, mainly due to literature source estimate uncertainties. Assuming lower

314   bound estimates for natural, agriculture/waste/landfills, and BBM sources *simultaneously* would

315   lead to FER of 8% or higher averaged during 2004-2011 (SI Figure S5). Yet, Figure 1 shows that

316   such high FER is inconsistent with the C_2H_6 data.

317
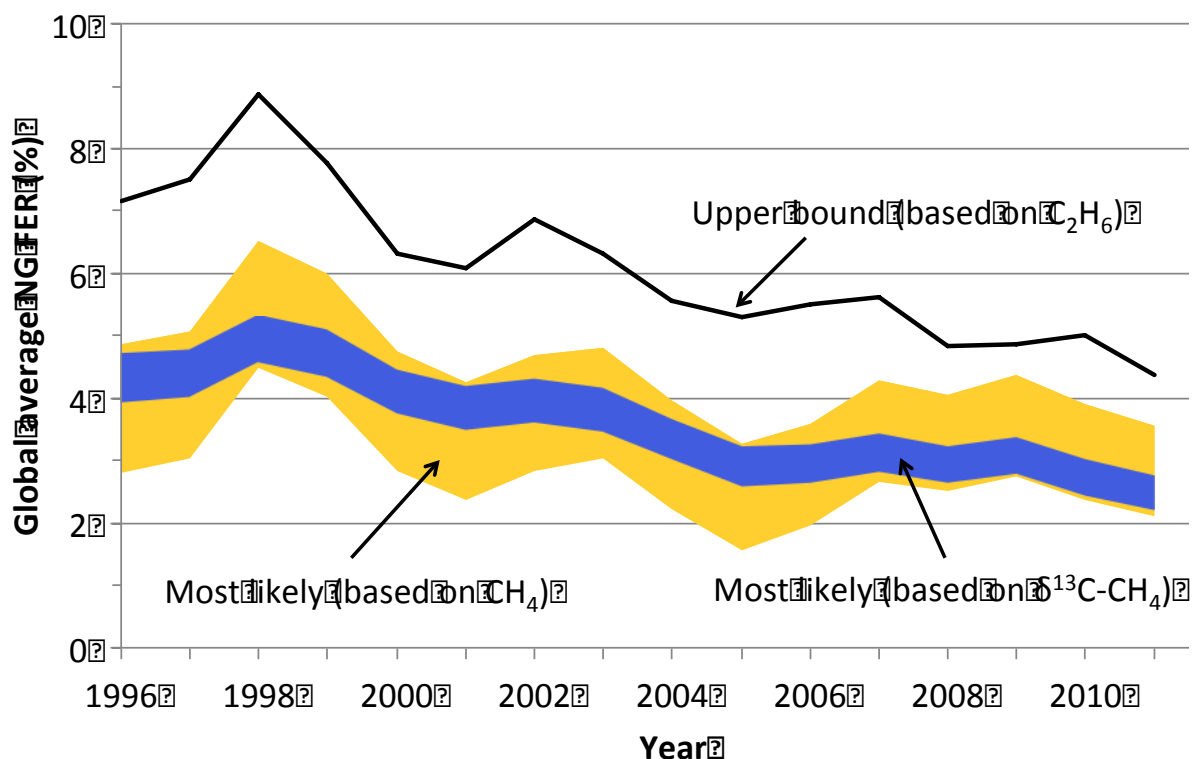
318

319   **Figure 1:** Summary of possible global NG fugitive emissions rates (FER) – in % of dry production

320   – based on a global mass balance using different tracer gases. The upper bound represents a

321   combination of assumptions from the literature including high global emissions (totaling 16.2 Tg

322   C_2H_6/yr on average since 2000 using UC-Irvine observations[13] and Rudolph[24] C_2H_6 lifetime

323   uncertainty) and low magnitude of other C_2H_6 sources (7.4 Tg C_2H_6/yr on average since 2000).

324   The orange and blue bands mark the range for CH_4 lifetimes between 9.1-9.7 years and mean

325   literature values of other CH_4 sources (totaling 467 Tg CH_4/yr on average since 2000 including

326   soil sink) using NOAA observations[19]. FER is shown for the longest consecutive observation time

327   series available (pre-1996 data are shown in SI Figures S5, S7).

328   Natural hydrocarbon seepage may be an additional significant source of atmospheric CH_4 and

329   C_2H_6 not currently accounted for in most top-down studies[17]. Visible macro-seeps, marine seepage,

330   micro-seepage,   and geothermal/volcanic areas may contribute between 40-60 Tg CH_4/yr and 2-

331   4 Tg C_2H_6/yr globally[59]. While not included in Figure 1, adding 40 Tg CH_4/yr and 2 Tg C_2H_6/yr

332   in the model would reduce FER by about two percentage points (constant over time). The

333   magnitude of the above seepage estimates have been challenged[13]. Yet, having excluded any

334   seepage in our main results (Figure 1) emphasizes that our FER may be overestimated.

335   The decline in global FER is 0.1 and 0.3 percentage points per year since 1985 based on most

336   likely (CH_4 and δ^{13}C-CH_4 observations) and upper bound results (C_2H_6 observations),

337   respectively. This assumes that the declines in measured C_2H_6 levels (or CH_4 growth rates[60]) are

338   attributed to NG emissions reductions. Kirschke *et al.*[17] find little if any long-term natural,

339   agriculture/waste/landfill, and BBM emissions reductions over this period. Kirschke *et al.*[17]

340   results, along with the findings presented here, suggest that the declines in measured mixing ratios

341   (or growth rates thereof) can be attributed to NG emissions reductions. This is also consistent with

342   recent top-down C_2H_6 studies[13,14] suggesting reductions in total FF emissions where Aydin *et al.*[14]

343   concluded that global declines in the C_2H_6 mixing ratios were due to decreased flaring and venting

344   of NG (see also SI Figure S8). Also, recent direct CH_4 measurements at 190 NG production sites

345   in the U.S. by Allen *et al.*[8] indicate lower overall CH_4 emissions from production (well pad)

346   activities than previous measurement data used in EPA's 2013 GHG inventory[51]. Note that

347   increased NG, oil, and coal production over time[61] was incorporated in the modeling presented

348   here. The FER decline may be less pronounced if oil and coal emissions per unit of production

349   also decreased since 1985. Atmospheric chemistry may also explain changes in CH_4 and C_2H_6

350   mixing ratios. However, Montzka *et al.*[62] recently found a small inter-annual atmospheric OH

351 variability of 2.3 ± 1.5% during 1998–2007, which suggests that increased sink strength is an

352 unlikely alternative explanation for declining FER.

Global 3D-model

354 Most-likely FER estimates from the mass balance are supported by the global chemistry

355 transport model TM5[26] and the spatial distribution of CH_4 mixing ratios as an indicator of source

356 strength[63]. Using three different FER scenarios ranging from about 2-6% FER (see SI Table S4

357 and Figure S9), the TM5 was used to simulate spatially distributed CH_4 sources and sinks from

358 1989-2011. As shown in Figure 2a, the medium FER scenario is a reasonable fit globally

359 throughout the 1990s (3-4% FER) compared to 3% and 5% in the box-model (SI Figure S5) for

360 CH_4 lifetimes (τ) of 9.7 and 9.1, respectively. In the 2000s, TM5 suggests a most likely FER of

361 ~3% dropping to just over 2% in 2010 compared to 2-4% in the box-model depending on τ. Given

362 that τ used in TM5 is approximately 9.45, most likely estimates of both models agree within one

363 percentage point FER.

364 The following spatial analysis is useful for investigating whether the *a priori* emissions source

365 attribution (Tables 1 and 2) is reasonable, or if – for instance – underestimated FER scenarios were

366 compensated by overestimated other source categories. Simulations and measurements across 41

367 latitudinal bands (intervals of 0.05 sine of latitude) are shown in Figure 2b as an indicator of the

368 inter-hemispheric gradient (for year 2000; see SI Figure S10 for additional years). The spatial fit

369 of simulations and measurements can be used as a proxy for the attribution of sources. About 96%

370 of NG CH_4 emissions in the emissions grid maps simulated with TM5 are released in the Northern

371 Hemisphere. The equivalent CH_4 emissions values in the Northern Hemisphere for oil, coal,

372 agriculture/waste/landfills, and natural sources are 91%, 88%, 82%, and 54%, respectively. The

373 observed difference between the most Southern (90°S-72°S) and Northern (72°N-90°N) latitudinal

374   band is 134 ppb (7.6% of the global average CH_4 mixing ratio) compared to 177 ppb (10.1%) in

375   the simulation (medium FER scenario) averaged over 1990-2010, which is qualitatively consistent

376   with previous studies[35,64]. This small North-South (N-S) gradient mismatch between observations

377   and simulation suggests that the simulated CH_4 estimates for each source category could be

378   plausible.

379
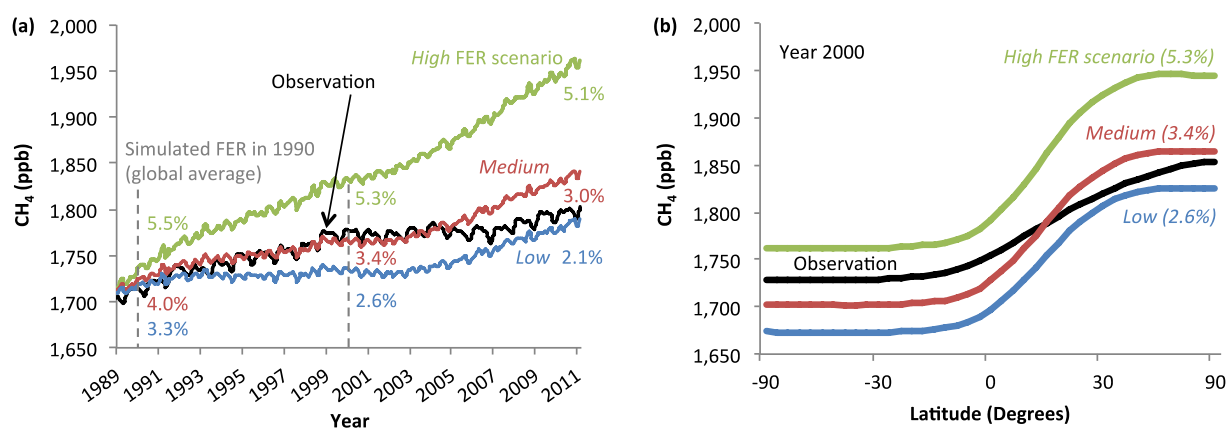
380

381   **Figure 2:** TM5 global average forward modeling results for three regionally and temporally

382   distinct FER scenarios (see SI Table S4 and Figure S9) as well as NOAA's measurements[19]. **(a)**

383   Global average dry air mole fractions; see[65,66] for estimating global averages from spatial

384   distributions. **(b)** CH_4 dry air mole fractions across 41 latitudinal bands in year 2000 (see SI Figure

385   S10 for additional years).

386   The inter-hemispheric gradient indicates that total emissions in the medium FER scenario (best

387   global fit in 2000; see Figure 2a) are too high in the North and too low in the South (relative to the

388   simulated *a priori* dataset). Also, the simulated inter-hemispheric gradient is significantly higher

389   than the observation in all FER scenarios. Because (i) reducing FER alone is not sufficient to match

390   the observed inter-hemispheric gradient, and (ii) coal and oil CH_4 totals are considered a low

391   estimate (i.e., Northern emissions could be even higher), misallocation of non-FF CH_4 emissions

392   across hemispheres must at least partially explain the N-S mismatch. This is consistent with

393   previous atmospheric inversions, which tend to reduce high latitudinal sources compensated by

394   increases at lower latitudes[35,64]. Tropical wetlands may be underestimated in particular[35]. Further

395   evidence is provided in the SI (section 3.2), which illustrates that NG (or other FFs) are unlikely

396   causes of the N-S mismatch between simulations and observations. Instead, seasonal observations

397   suggest that wetlands (a reduction in the North and an increase in the South) and/or

398   agriculture/waste/landfills (an increase in the North) were biased in the *a priori* estimates.

399   **Influence of FER on life cycle GHG emissions of power generation compared with coal**

400   The life cycle GHG emissions from power generation are frequently estimated to assess the

401   feasibility of replacing coal with NG to mitigate climate change[10,11,67–69]. Note, however, that other

402   comparisons, e.g., use as a transportation fuel[70], are also policy-relevant. Corresponding to

403   previous work[10,11,67–69], this study estimates the climate implications of NG in terms of CO_2-

404   equivalent (CO_2e) emissions per unit of generated electricity. This metric accounts for the

405   differences in cumulative radiative forcing of CH_4 relative to CO_2 over a given period – commonly

406   100 and 20 years – using global warming potentials (GWP)[71]. Figure 3 compares total life cycle

407   GHG emissions of power generation from coal and NG assuming 39% and 50% efficiency,

408   respectively. Given a GWP of 28 (100-yr period), and assuming 3% FER (i.e., the mean value of

409   the most likely FER range since 2000 from this study), total NG emissions are about 39% lower

410   than coal. After including climate-carbon feedbacks (CC FB), which account for the impact of the

411   GHGs on other gaseous and aerosol forcing species[71], this value decreases to 36% (GWP 34). The

412   FER would need to be 10% (excluding CC FB; 8.5% FER including CC FB) in order to reach the

413   same total emissions as coal (break-even point). However, over a 20-yr period, NG already breaks

414   even with coal at 3.4% FER, thus well within the most likely FER range in this study. Results for

415   GWP 84 (20-yr, no CC FB) are not shown in Figure 3 because differences are negligibly small

416   (3.5% break-even FER). Note that this coal-NG comparison excludes potential direct climate

417   effects from non-GHG climate forcers, such as sulfate aerosols from coal combustion, which may

418   have a cooling effect[2].

419
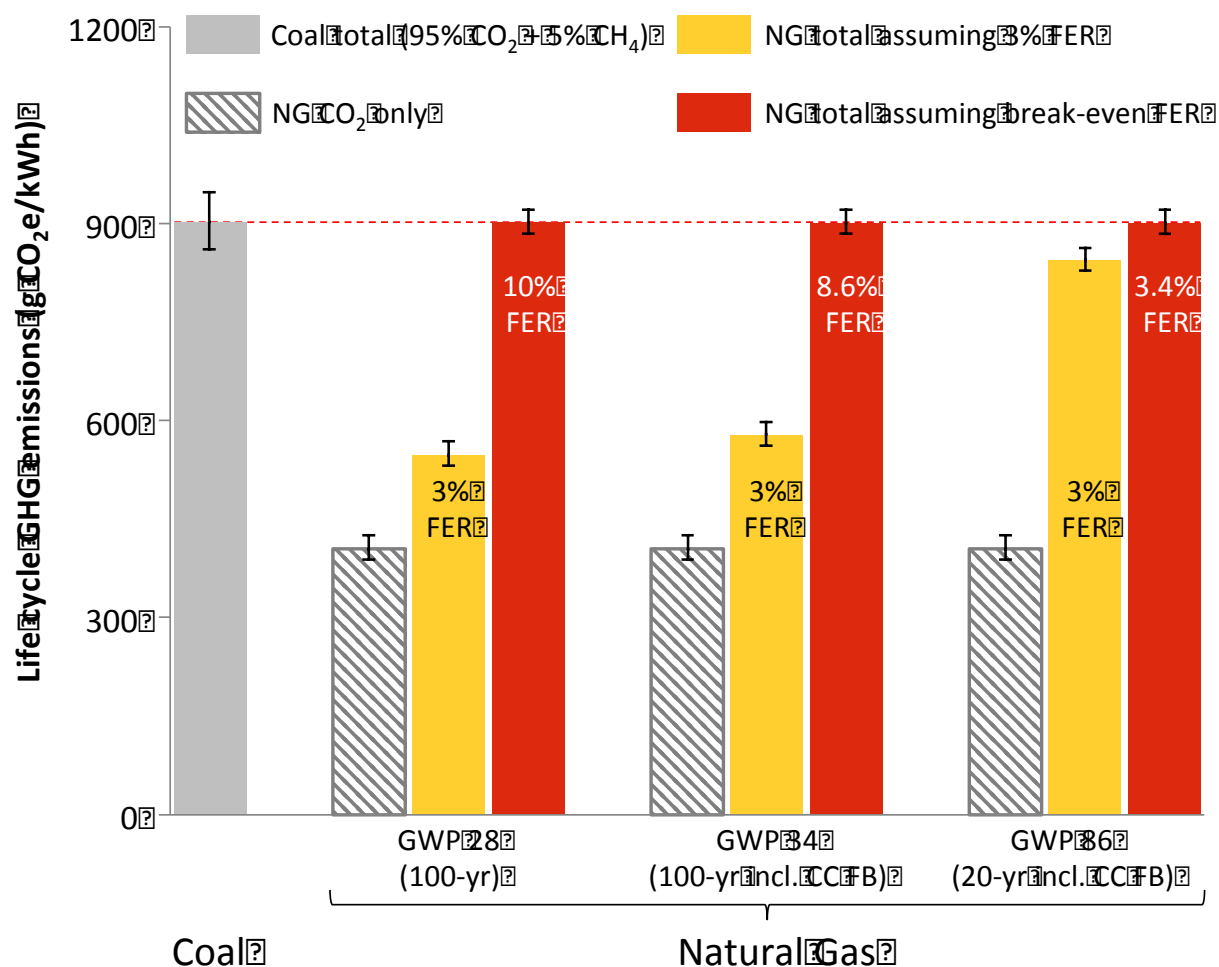
420   **Figure 3:** Comparison of life cycle GHG emissions of power generation from coal and NG

421   assuming 39% and 50% conversion efficiency, respectively. Literature estimates for coal[1,2,11] and

422   NG[1,2,10,72] CO_2 were used. Yellow and red columns assume 3% FER (mean value of most likely

423   FER range since 2000 from this study) and break-even FER (required to match coal emissions),

424   respectively, using 48 g CO_2e/kWh per percentage point FER from[68]. NG is shown for three

425   different global warming potentials (GWP; see text). Coal is shown for GWP 28 only because CH_4

426   contributes only 5% to total emissions. NG error bars include CO_2 only. Coal error bars pertain to

427   combined uncertainty in CO_2 and CH_4 emissions. CC FB: climate-carbon feedbacks (see text).

Discussion

429   The objective of this top-down study was to estimate global average FER related to the NG life

430   cycle in order to better understand whether recently reported high FER of 6-9%[1,4] are

431   representative of the larger NG industry. Using a global box-model and well-known quantities of

432   global average atmospheric CH_4, $\delta^{13}C$-CH_4, and C_2H_6 mixing ratios, the most likely FER was

433   found to be 2-4% since 2000, and currently (2006-2011) having an upper bound FER of 5%. Both

434   results are potentially overestimated because these estimates exclude highly uncertain emissions

435   from natural hydrocarbon seepage. Taking into account increasing NG (and other FF) production,

436   the FER (in % of dry production) has been declining steadily over time.

437   The box-model results (most likely FER of 2-4% since 2000) are consistent with those from 3D

438   modeling. The low magnitude of the difference in the inter-hemispheric gradient between

439   simulations and measurements (less than 5% of the global budget) indicates a minor bias in the

440   simulated emissions sources. The inter-hemispheric gradient and seasonal comparisons show that

441   an improved spatial emissions allocation includes (i) an emissions transfer from Northern to

442   Southern wetland emissions and/or (ii) increased Northern agriculture/waste/landfills emissions in

443   combination with FER lower than 2-4%. Thus neither the inter-hemispheric gradient nor the

444   seasonal comparisons suggest that a global average FER of 2-4% over the period 2000-2011 is too

445   low. This conclusion is subject to potential imprecision of the TM5 emissions transport model,

446   which may lead to uncertainties in the simulated spatial allocation of CH_4 emissions. However,

447   this is unlikely given the independent C_2H_6 based box-model upper bound FER of 5%.

448   The study results lead to both research recommendations and policy implications. A more formal

449   uncertainty analysis of key parameters (atmospheric lifetimes, natural emissions and NG

450   composition) would provide a more detailed characterization of FER uncertainties. This requires

451   composition data by well type (NG, oil) that are not currently available at this level of detail.

452   Policies aimed at providing such data, e.g., publishing international well sample data collected

453   from the oil and gas industry in a central database, would improve the accuracy of FER estimates.

454   The most likely global FER range (2-4%) is slightly higher than many recent bottom-up

455   estimates (1.1-3.2%; full life cycle) in the U.S. and elsewhere[10,51,68,73]; however, potentially

456   unaccounted natural seepage could reduce our estimate. Our most recent (2011) *global* upper

457   bound of 4.4% FER suggests that two recent high estimates of 6-9% in the U.S.[1,4] may be possible

458   at individual sites, but do not appear representative of the national average unless U.S. NG industry

459   practices are significantly worse than in the rest of the world. When used for power generation,

460   combined NG CH_4 and CO_2 emissions break even with coal at 8.6% FER using a 100-year CH_4

461   GWP (including CC FB), but the break-even is only 3.4% over 20 years (Figure 3). Thus, despite

462   our relatively low FER estimates, policies to further reduce fugitive emissions appear justified.

463   Shale gas production was too small globally (increasing from 1.5% of global production in 2007

464   to 5.9% in 2011[61]) to yield a signal *even if* FER from shale gas is higher than from conventional

465   NG. However, few bottom-up studies indicate significantly higher FER from shale compared to

466   conventional gas[68]. Local and regional top-down studies using field measurements can

467   complement global modeling. These may provide more basin specific FER estimates unattainable

468   with the current global observational network. The NG industry average FER estimates from this

469   work can be used as a reference, and basin specific studies may point to areas with local or regional

470   hot spots.

471

472   **Supporting Information**. Literature review of simulated non-FF emissions, observational data

473   description, additional box-model and 3D-model results, and comparison of GHG emissions

474   impacts from NG and coal power generation using global warming potentials. This material is

475   available free of charge via the Internet at http://pubs.acs.org.

476   **Present Addresses**

477   ♮ NOAA Earth Systems Research Laboratory, 325 Broadway GMD1, Boulder, CO 80305, United

478   States

479   **Author Contributions**

480   S.S. was responsible for study design, development of box-model and emissions inventory,

481   analysis of 3D-model results, and manuscript preparation. W.M.G. and H.S.M. helped with study

482   design, model analysis, and improved the manuscript. L.B. did 3D-modeling, helped with model

483   analysis, and improved the manuscript. All authors have given approval to the final version of the

484   manuscript.

492   (http://cdiac.ornl.gov/trends/otheratg/blake/blake.html). This research was made possible through

493   support from the Climate and Energy Decision Making (CEDM) center. This Center has been

494   created through a cooperative agreement between the National Science Foundation (SES-

495   0949710) and Carnegie Mellon University. The ERM Foundation-North America Sustainability

496   Fellowship has provided additional funding.

497   **Abbreviations**

498   CH_4, methane; C_2H_6, ethane; EF, emissions factor; FER, fugitive emissions rate (% of dry

499   production of NG); FF, fossil fuels (natural gas, oil, coal); GWP, global warming potential; NG,

500   natural gas.

501   **References**

502   1.   Howarth, R. W., Santoro, R. & Ingraffea, A. *Clim. Change* **106,** 679–690 (2011).

503   2.   Wigley, T. M. L. *Clim. Change* **108,** 601–608 (2011).

504   3.   Pétron, G. *et al. J. Geophys. Res.* **117,** D04304 (2012).

505   4.   Karion, A. *et al. Geophys. Res. Lett.* **40,** 4393–4397 (2013).

506   5.   Miller, S. M. *et al. Proc. Natl. Acad. Sci.* **110,** 20018–20022 (2013).

507   6.   Brandt, A. R. *et al. Sci.* **343 ,** 733–735 (2014).

508   7.   EPA. *Oil and Natural Gas Sector: Reconsideration of Certain Provisions of New Source*
509   *Performance Standards, Final Rule, 40 CFR Part 60*. (2013).
510   http://www.gpo.gov/fdsys/pkg/FR-2013-09-23/pdf/2013-22010.pdf

511   8.   Allen, D. T. *et al. Proc. Natl. Acad. Sci. U. S. A.* **110,** 17768–73 (2013).

512   9.   API/ANGA. *Characterizing Pivotal Sources of Methane Emissions from Natural Gas*
513   *Production: Summary and Analysis of API and ANGA Survey Responses*. (2012).

514   10.   Venkatesh, A., Jaramillo, P., Griffin, W. M. & Matthews, H. S. *Environ. Sci. Technol.* **45,**
515   8182–8189 (2011).

516   11.   Jiang, M. *et al. Environ. Res. Lett.* **6,** 034014 (2011).

517   12.   Gage, B. D. & Driskill, D. L. *Analyses of natural gases 1917-2007*. (2008).

518   13.   Simpson, I. J. *et al. Nature* **488,** 490–494 (2012).

519   14.   Aydin, M. *et al. Nature* **476,** 198–201 (2011).

520   15.   Levin, I. *et al. Nature* **486,** E3–E4 (2012).

521   16.   Miller, J. B. The carbon isotopic composition of atmospheric methane and its constraint
522   on the global methane budget. In *Stable Isot. Biosph. Interact.* (Flanagan, L. B.,
523   Ehleringer, J. R. & Pataki, D. E.) 288–310 (Elsevier, 2005).

524   17.   Kirschke, S. *et al. Nat. Geosci.* **6,** 813–823 (2013).

525   18.   Schwietzke, S., Griffin, W. M. & Matthews, H. S. Global bottom-up fossil fuel fugitive
526   methane and ethane emissions inventory for atmospheric modeling. *ACS Sustainable*
527   *Chem. Eng.* (2014). Accepted.

528   19.   ESRL. *CarbonTracker-CH4 documentation*. (2013).
529   http://www.esrl.noaa.gov/gmd/ccgg/carbontracker-ch4/documentation_obs.html#ct_doc

530   20.   Prinn, R. G., Huang, J., Weiss, R. F. & Cunnold, D. M. *Geophys. Res. Lett.* **32,** 2–5
531   (2005).

532   21.   Prather, M. J., Holmes, C. D. & Hsu, J. *Geophys. Res. Lett.* **39,** (2012).

533   22.   Naik, V. *et al. Atmos. Chem. Phys.* **13,** 5277–5298 (2013).

534   23.   Voulgarakis, A. *et al. Atmos. Chem. Phys.* **13,** 2563–2587 (2013).

535   24.   Rudolph, J. *J. Geophys. Res. Atmos.* **100,** 11369–11381 (1995).

536   25.   Hartmann, D. L. *et al.* Observations: Atmosphere and Surface. In *Clim. Chang. 2013*
537   *Phys. Sci. Basis. Contrib. Work. Gr. I to Fifth Assess. Rep. Intergov. Panel Clim. Chang.*
538   (Stocker, T. F. et al.), (Cambridge University Press, 2014).

539   26.   Krol, M. *et al. Atmos. Chem. Phys.* **5,** 417–432 (2005).

540   27.   Bruhwiler, L. *et al.* CarbonTracker-CH4: An assimilation system for estimating emissions
541   of atmospheric methane. *Atmos. Chem. Phys.* (2013). Submitted.

542   28.   Fung, I., Prather, M., John, J., Lerner, J. & Matthews, E. *J. Geophys. Res.* **96,** 13033–
543   13065 (1991).

544 29. Lassey, K. R., Lowe, D. C. & Manning, M. R. *Global Biogeochem. Cycles* **14,** 41–49
545   (2000).

546 30. Sriskantharajah, S. *et al. Tellus B; Vol 64* (2012).
547   http://www.tellusb.net/index.php/tellusb/article/view/18818

548 31. Schoell, M. *Am. Assoc. Pet. Geol. Bull.* **67,** 2225–2238 (1983).

549 32. Michel, S. E. Institute of Arctic and Alpine Research (INSTAAR), University of
550   Colorado, Boulder. *Personal communication*. (2014).

551 33. Miller, J. B. *et al. J. Geophys. Res. Atmos.* **107,** ACH 11–1–ACH 11–15 (2002).

552 34. EIA. *International Energy Statistics*. (2013).
553   http://www.eia.gov/cfapps/ipdbproject/iedindex3.cfm?tid=2&pid=38&aid=12&cid=region
554   s&syid=1980&eyid=2011&unit=BKWH

555 35. Mikaloff Fletcher, S. E., Tans, P. P., Bruhwiler, L. M., Miller, J. B. & Heimann, M.
556   *Global Biogeochem. Cycles* **18,** GB4004 (2004).

557 36. Bousquet, P. *et al. Nature* **443,** 439–43 (2006).

558 37. Chen, Y.-H. & Prinn, R. G. *J. Geophys. Res. Atmos.* **111,** (2006).

559 38. Wang, J. S. *et al. Global Biogeochem. Cycles* **18,** (2004).

560 39. IPCC. *Climate Change 2001: The Physical Science Basis. Contribution of Working Group*
561   *I to the Third Assessment Report of the Intergovernmental Panel on Climate Change.*
562   *Chapter 6*. (2001).

563 40. Wuebbles, D. J. & Hayhoe, K. *Earth-Science Rev.* **57,** 177–210 (2002).

564 41. Ridgwell, A. J., Marshall, S. J. & Gregson, K. *Global Biogeochem. Cycles* **13,** 59 (1999).

565 42. Bergamaschi, P. *et al. J. Geophys. Res.* **112,** 1–26 (2007).

566 43. Janssens-Maenhout, G. *et al. EDGAR-HTAP: a harmonized gridded air pollution*
567   *emission dataset based on national inventories*. (2012).

568 44. Matthews, E., Fung, I. & Lerner, J. *Global Biogeochem. Cycles* **5,** 3 (1991).

569 45. Giglio, L., Van Der Werf, G. R., Randerson, J. T., Collatz, G. J. & Kasibhatla, P. *Atmos.*
570   *Chem. Phys.* **6,** 957–974 (2006).

571 46. Van Der Werf, G. R. *et al. Atmos. Chem. Phys. Discuss.* **6,** 3175–3226 (2006).

572   47.   GFED. *Global Fire Emissions Database*. (2013). http://www.globalfiredata.org/

573   48.   Elvidge, C. D. *et al. Energies* **2,** 595–622 (2009).

574   49.   Elvidge, C. D., Baugh, K. E., Ziskin, D., Anderson, S. & Ghosh, T. *Estimation of Gas*
575   *Flaring Volumes Using NASA MODIS Fire Detection Products*. (2011).

576   50.   IPCC. *2006 IPCC Guidelines for National Greenhouse Gas Inventories, Prepared by the*
577   *National Greenhouse Gas Inventories Programme*. *Agric. For. Other L. Use* **4,** (IGES,
578   2006).

579   51.   EPA. *Inventory of U.S. Greenhouse Gas Emissions and Sinks: 1990 – 2011*. (2013).
580   http://www.epa.gov/climatechange/ghgemissions/usinventoryreport.html

581   52.   Wilson, D., Fanjoy, J. & Billings, R. *Gulfwide Emission Inventory Study for the Regional*
582   *Haze and Ozone Modeling Effort*. (2004).

583   53.   Wilson, D. *et al. Year 2008 Gulfwide Emission Inventory Study*. (2010).

584   54.   EPA. *Reducing Methane Emissions From Coal Mines in China: The Potential for*
585   *Coalbed Methane Development*. (1996).

586   55.   CIRI. *China Coal Industry Yearbook 2009*. (2011).

587   56.   EPA. State Inventory and Projection Tool. (2012).
588   http://www.epa.gov/statelocalclimate/resources/tool.html

589   57.   Fung, I., Matthews, E. & Lerner, J. *Abstr. Pap. Am. Chem. Soc.* **193,** 6–GEOC (1987).

590   58.   Kaplan, J. O. *Geophys. Res. Lett.* **29,** 3–6 (2002).

591   59.   Etiope, G. & Ciccioli, P. *Science (80-.).* **323,** 478 (2009).

592   60.   Nisbet, E. G., Dlugokencky, E. J. & Bousquet, P. *Sci.* **343 ,** 493–495 (2014).

593   61.   EIA. *U.S. Energy Information Administration*. (2014). www.eia.gov

594   62.   Montzka, S. A. *et al. Science* **331,** 67–69 (2011).

595   63.   Dlugokencky, E. J., Nisbet, E. G., Fisher, R. & Lowry, D. *Philos. Trans. R. Soc. - Ser. A*
596   *Math. Phys. Eng. Sci.* **369,** 2058–2072 (2011).

597   64.   Houweling, S., Kaminski, T., Dentener, F., Lelieveld, J. & Heimann, M. *J. Geophys. Res.*
598   **104,** 26137–26160 (1999).

599   65.   Dlugokencky, E. J., Steele, L. P., Lang, P. M. & Masarie, K. A. *J. Geophys. Res.* **100,**
600   23103 (1995).

601   66.   Masarie, K. A. & Tans, P. P. *J. Geophys. Res.* **100,** 11593 (1995).

602   67.   NETL. *Life Cycle Greenhouse Gas Inventory of Natural Gas Extraction, Delivery and*
603   *Electricity Production*. (2011).

604   68.   Weber, C. L. & Clavin, C. *Environ. Sci. Technol. Technol.* **46,** 5688–5695 (2012).

605   69.   Burnham, A. *et al. Environ. Sci. Technol.* **46,** 619–627 (2012).

606   70.   Alvarez, R. A., Pacala, S. W., Winebrake, J. J., Chameides, W. L. & Hamburg, S. P. *Proc.*
607   *Natl. Acad. Sci. U. S. A.* **109,** 6435–40 (2012).

608   71.   Myhre, G. *et al.* Anthropogenic and Natural Radiative Forcing. In *Clim. Chang. 2013*
609   *Phys. Sci. Basis. Contrib. Work. Gr. I to Fifth Assess. Rep. Intergov. Panel Clim. Chang.*
610   (Stocker, T. F. et al.) (Cambridge University Press, 2014).

611   72.   Jaramillo, P., Griffin, W. M. & Matthews, H. S. *Environ. Sci. Technol.* **41,** 6290–6296
612   (2007).

613   73.   Dienst, C. *et al. Treibhausgasemissionen des russischen Exportpipeline System –*
614   *Ergebnisse und Hochrechnungen empirischer Untersuchungen in Russland*. (2004).

615

616   **TOC/Abstract art**

617